Available online at www.sciencedirect.com
ScienceDirect
Biochemical and Biophysical Research Communications 349 (2006) 50–58
BBRC
www.elsevier.com/locate/ybbrc

Mouse lymphomas caused by an intron-splicing donor site deletion of the *FasL* gene

Cheng-Chun Wang, Qi Zeng, Le-Ann Hwang, Ke Guo, Jie Li, Hwee Chien Liew, Wanjin Hong *

Institute of Molecular and Cell Biology, 61 Biopolis Drive, Singapore 138673, Singapore

Received 18 July 2006
Available online 22 August 2006

Abstract

A spontaneous lymphoma was detected in mice, which was caused by a recessive autosomal mutation. The genetic basis was revealed to be a 5-bp deletion at the splicing donor site of the first intron of the *FasL* gene, resulting in aberrant transcripts coding for non-functional proteins. This mutation of the *FasL* gene caused development of lymphoma in all four mouse genetic backgrounds tested and the lymphoma was characterized by an expansion of leucocytes that were $TCR^{+}CD3^{+}B220^{+}CD19^{-}CD4^{-}CD8^{-}$. Accordingly, severe splenomegaly developed in the mutant mice. Interestingly, thymic hyperplasia was observed in mutant mice at later stages. These results underscore the functional importance of the splicing donor site in the function of the *FasL* gene and provide an independent evidence for a role of FasL in normal development of lymphocytes. The mutant mice offer another genetically defined mouse model for further studies of the role and mechanism of action of FasL.

Keywords: FasL; Lymphoma; Intron; mRNA splicing; Lymphyocyte

Fas ligand (FasL) is a type II integral membrane protein of the tumor necrosis factor (TNF) superfamily [1] that can induce apoptosis in Fas-expressing cells [1,2]. Binding of FasL to Fas triggers recruitment of the death domain-containing adaptor protein FADD to the cytoplasmic domain of Fas followed by recruitment and activation of caspase-8 [3,4], which eventually leads to cell death. The Fas–FasL signaling mediates activation-induced cell death to suppress excessive expansion of chronically stimulated futile cells and autoreactive cells [5,6]. FasL may also be involved in establishing and/or maintaining immune-privilege in the eyes and the testis [7].

Unlike other members of the TNF family whose engagements with receptors are somewhat promiscuous, the FasL–Fas interaction seems to be extremely specific and exclusive. Ablation of either *Fas* or *FasL* results in almost identical phenotypes [8–10].

Study of the FasL–Fas function is initiated by the natural mutations *lpr* and *gld* that cause lymphoproliferative diseases in mice. *gld* is a point mutation in *FasL* while *lpr* is resulted from a transposon insertion into the second intron of the *Fas* gene [11,12]. Another mutation lpr^{cg} is a point mutation in *Fas* that causes a substitution of isoleucine for asparagine [13]. Recently, multiple mutations in human *FAS* gene have been reported in patients with an autoimmune lymphoproliferative syndrome (ALPS) [6,14–17]. On the contrary, *gld* remains the only natural mutation in *FasL* so far and no mutation in this gene has been reported yet in human diseases.

We report here a novel spontaneous mutation in the murine *FasL* that causes loss-of-function of the gene and results in development of lymphomas.

Materials and methods

Histology, immunofluorescence, flow cytometry, and Western blotting analysis. Organs were fixed with 4% paraformaldehyde (PFA) in PBS and

* Corresponding author. Fax: +65 6779 1117.
E-mail address: mcbhwj@imcb.a-star.edu.sg (W. Hong).

0006-291X/$ - see front matter © 2006 Elsevier Inc. All rights reserved.
doi:10.1016/j.bbrc.2006.07.215

embedded in paraffin. Sections were stained with hematoxylin and eosin. For immunofluorescence, PFA (kidney) or acetone (lung)-fixed cryosections as well as paraffin (liver) sections were used. IgG deposits in glomeruli were detected directly with a FITC-conjugated goat anti-mouse IgG antibody (Jackson ImmunoResearch Laboratories). To detect the B220 antigen, sections were stained sequentially with a rat anti-mouse CD45R/B220 monoclonal antibody (BD PharMingen) and a secondary FITC (liver) or Texas Red (lung)-conjugated goat anti-rat IgG antibody (Jackson ImmunoResearch Laboratories). We followed a protocol from BD PharMingen for flow cytometry analysis. Splenocytes were collected by squeezing spleen segments with the head of a 5 ml syringe. Red cells were removed by incubating the cell mixture at 37 °C for 5 min in a lysing buffer (0.16 M NH_4Cl, 0.17 M Tris–Hcl, pH 7.65). Fc receptors were blocked with a rat anti-mouse CD16/CD32 monoclonal antibody before staining with PE or FITC-conjugated specific antibodies. After being washed twice with a staining/washing buffer (PBS supplemented with 1% FBS and 0.1% sodium azide), cells were scanned for fluorescence with a FACScan cytometry from BD PharMingen. All antibodies used in this study were purchased from BD PharMingen. For Western blotting, 0.01 μl of serum from each mouse (5-month-old male) was used and a peroxidase-conjugated goat anti-mouse IgG or IgM antibody (Jackson ImmunoResearch Laboratories) was employed to detect γ chain or μ chain. Quantitative analysis was carried out with a GS-800 calibrated densitometer from Bio-Rad.

Genetic mapping, sequence and genotype analysis. Tumor mice originally on a Black Swiss and 129/Sv mixed background were bred onto a Balb/c background for two generations. Four tumor mice and two non-tumor control littermates bearing 75% of the Balb/c genome were then subjected to simple-sequence length polymorphism (SSLP) analysis by PCR with 120 microsatellite markers at a resolution of about 10 centi-Morgans (cM). The SSLP analysis service was provided by the Australia Genome Research Facility. The rationale was that the tumorgenic mutation must have derived from either the 129/Sv or the Black Swiss genome but not the Balb/c genome. Two markers, namely *D1Mit14* and *D1Mit36*, were found to be of homozygous 129/Sv origin in all tumor mice but of heterozygous origins in the two non-tumor mice, with one allele from Balb/c in each mouse. The mutation is thus linked to these two markers. To sequence the coding exons and exon–intron boundaries of the FasL gene, we amplified genomic DNA with the following primers: 1F (5′-AGA GTTCTGTCCTTGACACCTGAG-3′) and 1R (5′-ATGGGCCATAGC AAGTCCCTACT-3′); 2F (5′-GTGTGGCTAAACCCTAACTCGGG-3′) and 2R (5′-GAAGAGTCAAAAGCTCCTCAGGG-3′); 3F (5′-GATGG GATTTAGAGTCCTATCGAGA-3′) and 3R (5′-GGATGGTCTTGAG TGATAACTACAG-3′); 4F (5′-AAGGGATGCATGTCAGGTGTGTG A-3′) and 4R (5′-CAAGACAATATTCCTGGTGCCCATG-3′).

PCR was performed with the Advantage II polymerase from BD Clontech. Reaction conditions were: 3 min at 95 °C followed by 35 cycles of 30 s at 94 °C, 10 s at 65 °C (60 °C for exon 3) and 60 s at 68 °C. PCR

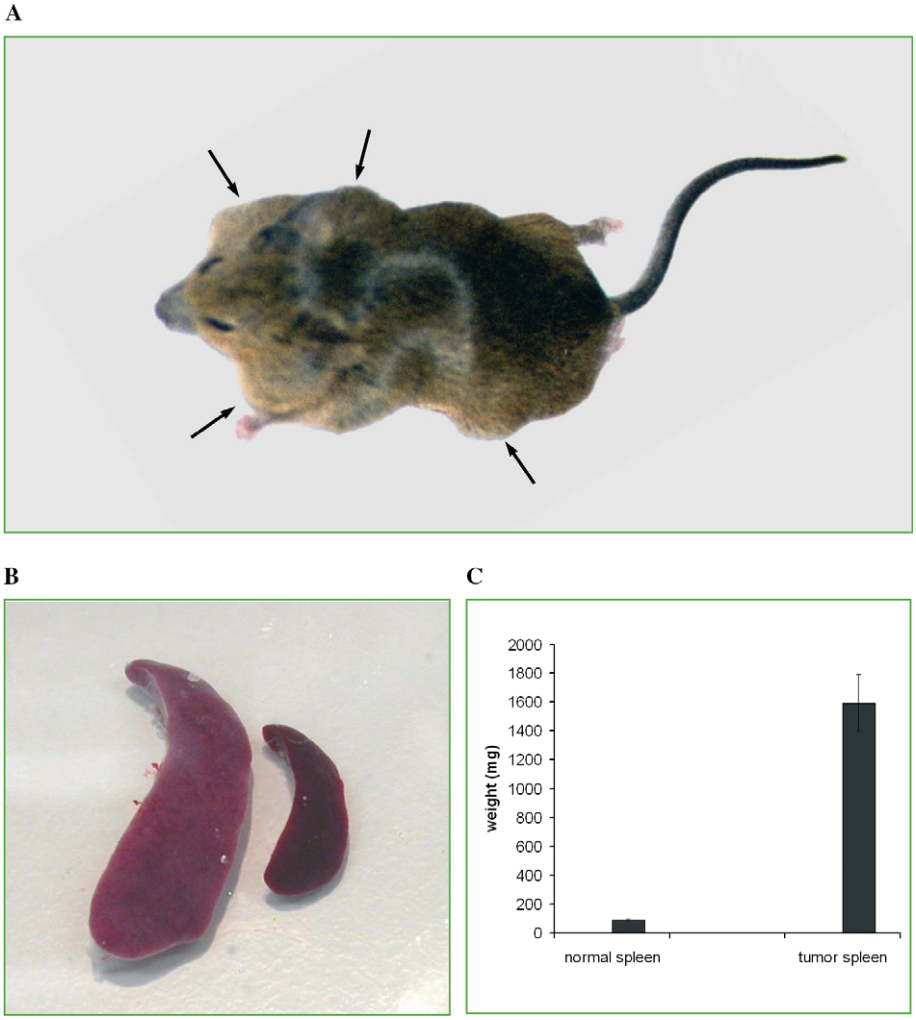

Fig. 1. Severe lymphomas caused by an spontaneous mutation in mice. (A) Overview of a 5-month-old mouse showing enlarged lymph nodes as indicated by arrows. (B) An enlarged spleen (left) from a tumor mouse is compared with a spleen (right) from a normal mouse. (C) The average weight of spleens of 5-month-old female tumor mice and sex-matched non-tumor littermates. $n = 4$, $P < 0.01$.

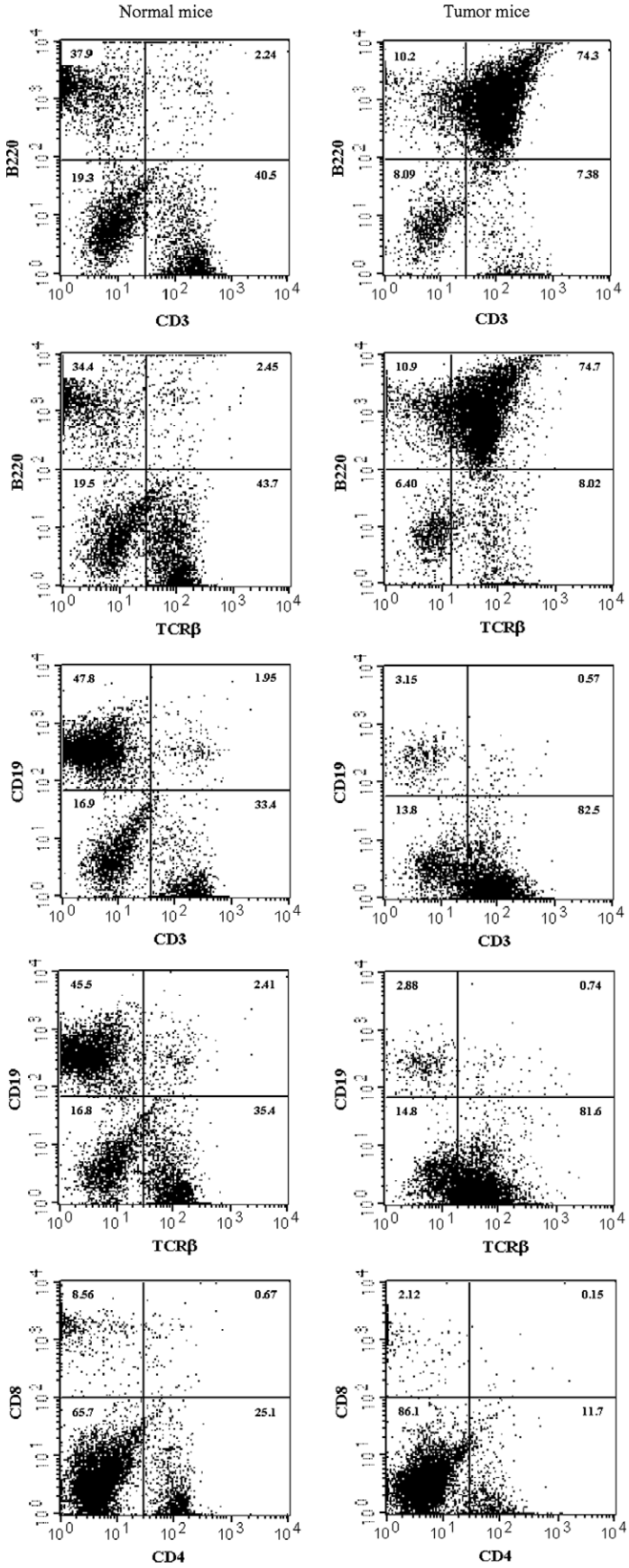

Fig. 2. Flow cytometry analysis of splenocytes derived from tumor mice and normal mice. Splenocytes derived form normal mice (left panels) and tumor mice (right panels) of 5-month-old were analyzed by flow cytometry and an unusual population of $TCR^{+}CD3^{+}B220^{+}CD19^{-}CD4^{-}CD8^{-}$ leukocytes were expanded in the tumor mice.

fragments were subjected to sequencing with the PCR primers shown above. To determine the genotype of littermates from heterozygote-heterozygote mating, toe and/or tail samples were digested with a lysis buffer (10 mM Tris–Hcl, pH 8.5, 50 mM KCl, 2 mM $MgCl_2$, 0.45% Nonidet P40, 0.45% Tween 20, and 200 μg/ml proteinase K) at 65 °C overnight. After inactivating residual proteinase K at 85 °C for 1 h, tissue lysate were used directly for PCR with the HotStarTaq master mix kit form Qiagen. Reaction conditions were 15 min at 95 °C followed by 35 cycles of 30 s at 94 °C, 10 s at 65 °C, and 20 s at 72 °C. PCR primers were forward (5′-CC ACCTGCAGAAGGAACTGGCA-3′) and reverse (5′-ATGGGCCATA GCAAGTCCCTACT-3′). PCR products were resolved on a 10% polyacrylamide gel.

mRNA preparation, RT-PCR and Northern blotting analysis. Splenocytes were cultured for 2 days at a concentration of 2×10^6 cells/ml in RPMI 1640 supplemented with 10% fetal calf serum, 50 μM β-mercaptoethanol, 1.5 μg/ml Con A, and 20 ng/ml interleukin-2. The blasts were then harvested and cultured for four more hours in RPMI 1640 containing 10 ng/ml PMA and 500 ng/ml ionomycin. Total RNA was isolated with the RNeasy midi kit from Qiagen and mRNA enrichment was carried out with an oligo(dT)-cellulose kit from New England Biolabs. cDNA was synthesized with an AMV reverse transcriptase form Promega, using oligo$(dT)_{15}$ as a primer. PCR was performed with the HotStarTaq master mix kit form Qiagen. Reaction conditions were 15 min at 95 °C followed by 35 cycles of 30 s at 94 °C, 20 s at 65 °C and 150 s at 72 °C. PCR primers were forward (5′-AGAGTTCTGTCCTTGACACCTGAG-3′) and reverse (5′-GGATAGCTGACCTGTTGGACCTTG-3′). PCR products were separated on a 1% agarose gel and individual fragments were extracted with the QIAEX II kit before being subjected to sequence analysis. Northern blotting was carried out with the Hybond-XL membrane as instructed by the manufacturer. The RT-PCR fragment produced with mRNA from wild-type spleen blasts was labeled with [α-^{32}P]dCTP and used as probe. Hybridization was done in the ExpressHyb buffer from BD Clontech as directed.

Results

An autosomal recessive mutation causes lymphomas in mice

When analyzing the *VAMP8* knockout mice [21], we noted that some mice developed lymphomas. The tumor phenotype, however, was not a result from the depletion of VAMP8 because lymphomas developed in $VAMP8^{-/-}$ and $VAMP8^{+/-}$ mice as well as in $VAMP8^{+/+}$ mice. We then crossed $VAMP8^{+/+}$ tumor mice, which were maintained on a 129Sv and C57BL/6 mixed background, onto three strains of wild-type mice, namely 129SvJ, C3H/HeJ, and Balb/c, for two to three generations. About a quarter of offspring from carrier to carrier mating were tumor

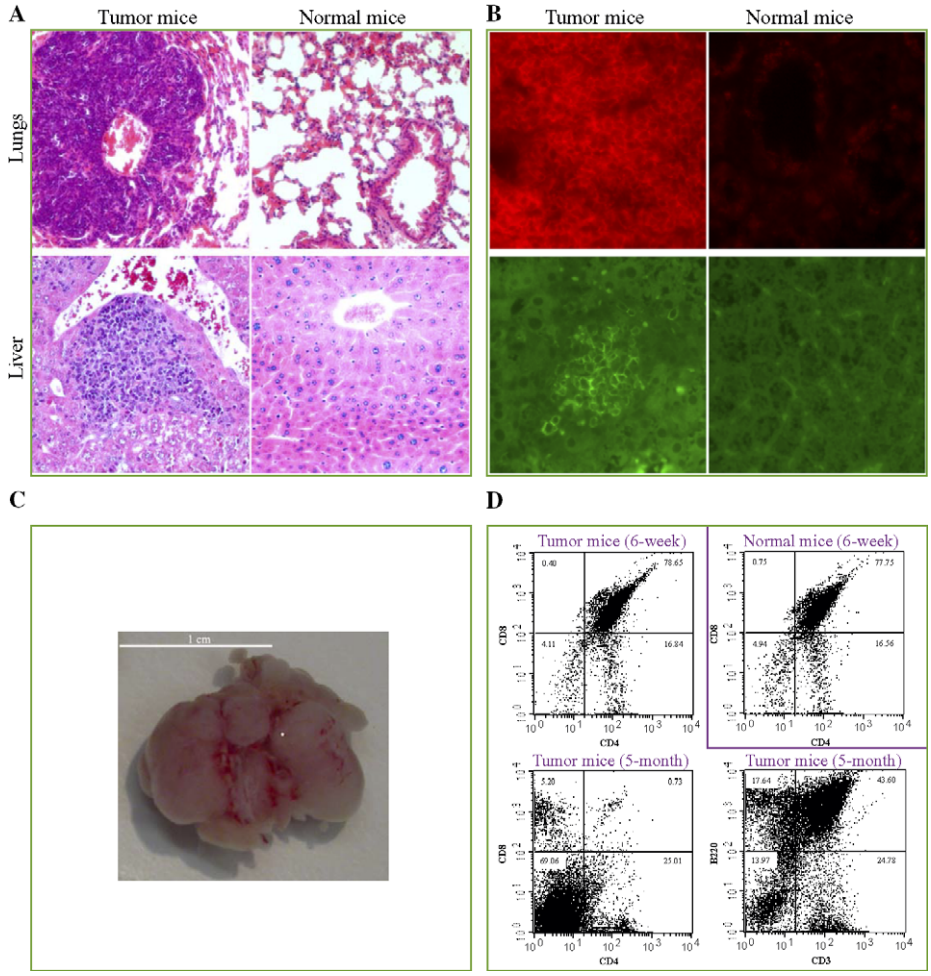

Fig. 3. Spread of lymphomas into thymus and non-lymphoid tissues. (A) H&E staining showing spread of lymphomas into the lung and liver. (B) Immunofluorescent staining for B220/CD45R showing that most leukocytes in the lung and liver of tumor mice are B220-positive. (C) Enlarged thymus from a 5-month male tumor mouse. The thymus weighed 1.05 g. (D) Flow cytometry analysis of thymocytes from 6-week and 5-month-old mice.

mice, regardless of genetic backgrounds. Tumor mice were evenly distributed between both sexes. Based on these observations, we concluded that the lymphoma is caused by an autosomal recessive mutation.

The lymphoma characteristics indicate a possible disruption of the FasL–Fas signaling pathway

Affected mice developed severe splenomegaly and lymphadenopathy (Fig. 1). Spleen enlargement was obvious from 6 weeks of age. By 9–10 weeks, tumor mice became evident with their bumping cervical lymph nodes. More than half of suffering mice died within four months and few survived beyond one year of age. Spleens of 5-month-old tumor mice were about 10–20 times larger than normal spleens (Fig. 1).

Flow cytometry analysis revealed a dramatic expansion of an unusual leukocyte population that was $TCR^{+}CD3^{+}B220^{+}CD19^{-}CD4^{-}CD8^{-}$. This population accounted for less than 3% of total splenocytes in normal mice but increased from about 5% at 6 weeks to over 70% at 5 months in lymphoma mice (Fig. 2).

Thymuses of tumor mice were not globally affected in mice younger than two months but started to grow from the end of the third month. By the age of 5–6 months, a tumor thymus could weigh more than 1 g (Fig. 3C) when the thymus in normal mice almost disappeared due to progressive atrophy. In contrast to 6-week thymocytes, which were mostly $CD4^{+}CD8^{+}$ cells in both normal and tumor mice, the majority of thymocytes from old tumor mice were $CD4^{-}CD8^{-}$ and $CD3^{+}B220^{+}$ (Fig. 3D), suggesting that the enlargement of the tumor thymus was a consequence of re-populating by the abnormal leukocytes.

The lymphoma could spread into non-lymphoid organs in old mice. Nodular lymphoid deposits were frequently found in liver and lungs (Fig. 3A). Apparently, the lymphoid cells in these organs were the abnormal cells since they were mostly B220-positive (Fig. 3B). Lymphocyte infiltration into lungs and liver was more severe on the Balb/c background than on the 129SvJ or the C3H/HeJ background. Spread of lymphoma cells into the kidney and ovary was also occasionally observed.

No lymphoma developed in nude mice that had been administered with tumor splenocytes via the tail vein. This

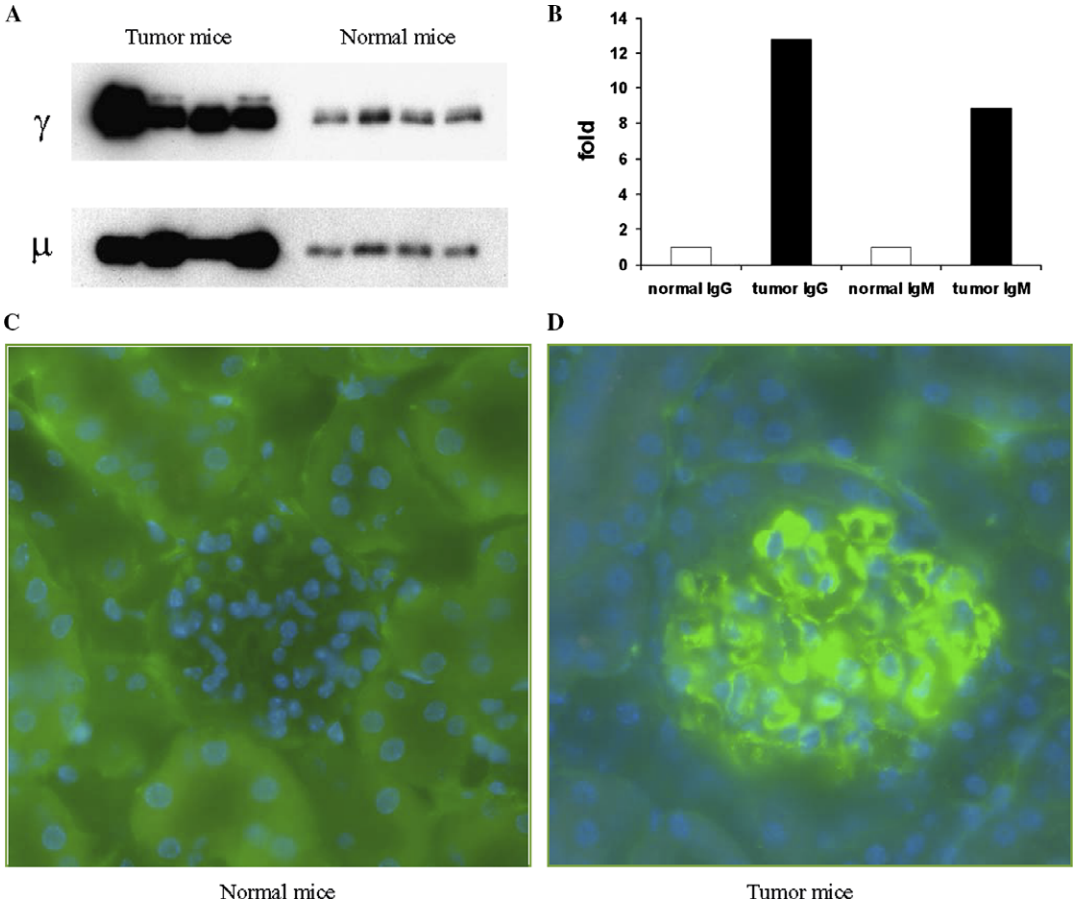

Fig. 4. Hyper-gammaglobulinemia of tumor mice. (A) Western-blotting analysis of serum IgG (γ chain) and IgM (μ chain) from 5-month-old mice. (B) Quantitative analysis of the Western blotting results shown in (A) with a densitometer. The total amount of serum IgG and IgM of four normal mice are arbitrarily defined as onefold. (C and D) Immunofluorescent staining for IgG in glomeruli of normal mice (C) tumor mice (D). Significant IgG deposits were detected in the glomeruli of tumor mice. The size of the glomerulus was also noticeably increased in tumor mice. The higher background labeling of kidney tubules surrounding the glumerulus of the normal mouse is due longer exposure time (as to show the negative signal of IgG in the glumerulus).

suggests that the lymphoma was not fully transformed and it might have resulted from a defect in apoptosis.

The Lymphoma phenotype described so far is very similar to those observed in *Fas* or *FasL* knockout mice. More over, like the FasL-null mice, our mice also exhibited hypergammaglobulinemia (Fig. 4). Serum IgG and IgM were increased by about 12 and 8 times, respectively, in tumor mice (Figs. 4A and B). Significant IgG deposits were also detected in glomeruli of our tumor mice (Fig. 4C). This phenotype is reminiscent of a possible disruption of the Fas–FasL signaling pathway in our mutant mice.

The lymphoma is caused by a 5-bp deletion at the first exon–intron boundary of FasL

To pinpoint the tumorgenic mutation, we performed a genetic mapping by analyzing simple-sequence length polymorphism (SSLP). A preliminary PCR screen showed that the lymphoma phenotype was tightly linked to two markers, namely *D1Mit14* and *D1Mit36*, which are located on chromosome 1 at the positions of 82 and 91.8 cM, respectively. Since *FasL* (on chromosome 1 at the position of 85 cM) is located between these two markers and the phenotype of the mutant mouse strikingly resembled that of the FasL-null mice, we then sequenced the coding exons and exon–intron boundaries of this gene. We found that five nucleotides at the splicing donor site in the first intron were deleted in lymphoma mice (Fig. 5). We designated this mutant allele as $FasL^{del}$, in contrast to the wild-type allele *FasL*. We found that all mice homozygous for $FasL^{del}$ developed tumors while all non-tumor mice were either heterozygous or homozygous for the wild-type allele (Fig. 5B).

To determine the molecular consequence of the deletion, we performed a RT-PCR analysis of spleen mRNA isolated from tumor mice and non-tumor mice. While a single neat band was produced with mRNA derived from wild-type mice, three major bands and a minor band were detected in mRNA derived from tumor mice (Fig. 6A). Sequence analysis showed that three aberrant transcripts in the tumor mice were generated from cryptic splicing sites in exon 1 and intron 1 (Fig. 6B) while the largest transcript remained the first intron intact and were the major transcript detected by Northern-blot analysis (Fig. 6D). The splicing between other exons was not altered. These transcripts were predicted to produce three polypeptides that lacked either the transmembrane domain, or the Fas-binding TNF domain or both (Fig. 6C). As expected, there was no surface FasL expressed on tumor T cells (Fig. 6E).

FasL is known to induce apoptosis of Fas-expressing cells. One might expect to see more Fas-expressing lymphocytes in $FasL^{del}/FasL^{del}$ mice. This was indeed the case. There were not only more cells expressing Fas, the expression level was also substantially higher in tumor mice than in normal mice. When gated at 10^1, about 55–60% of normal splenocytes were Fas-positive. This number went up to about 90% in tumor mice (Fig. 7). The $CD3^+B220^+$ cells

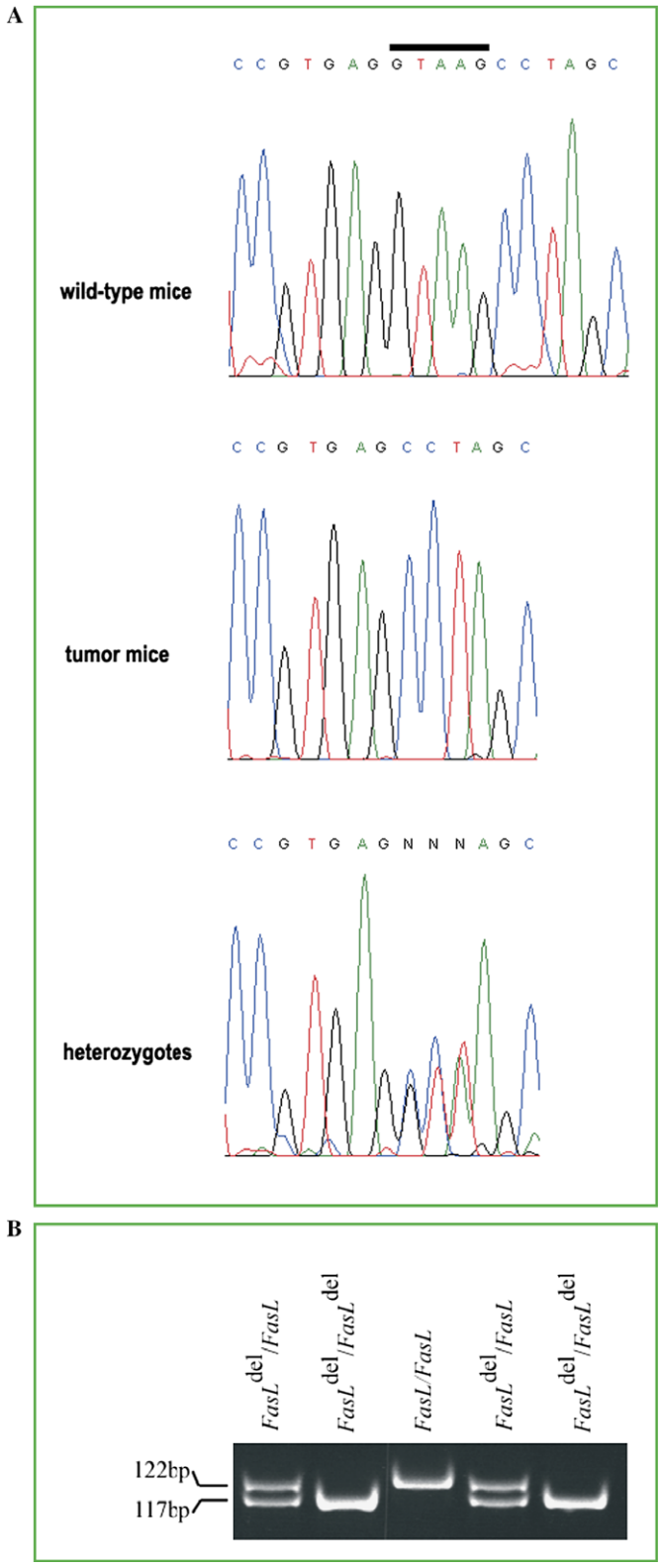

Fig. 5. A deletion of 5-bp in the *FasL* gene. (A) Sequence analysis of genomic DNA from different mice. Five nucleotides (over-lined) are deleted in the mutant allele. (B) Genotype analysis by PCR. The wild-type allele produces a fragment of 122 bp while the mutant allele yields a band of 117 bp. All tumor mice are homozygous for the mutant allele and non-tumor mice are either homozygous for the wild-type allele or heterozygous.

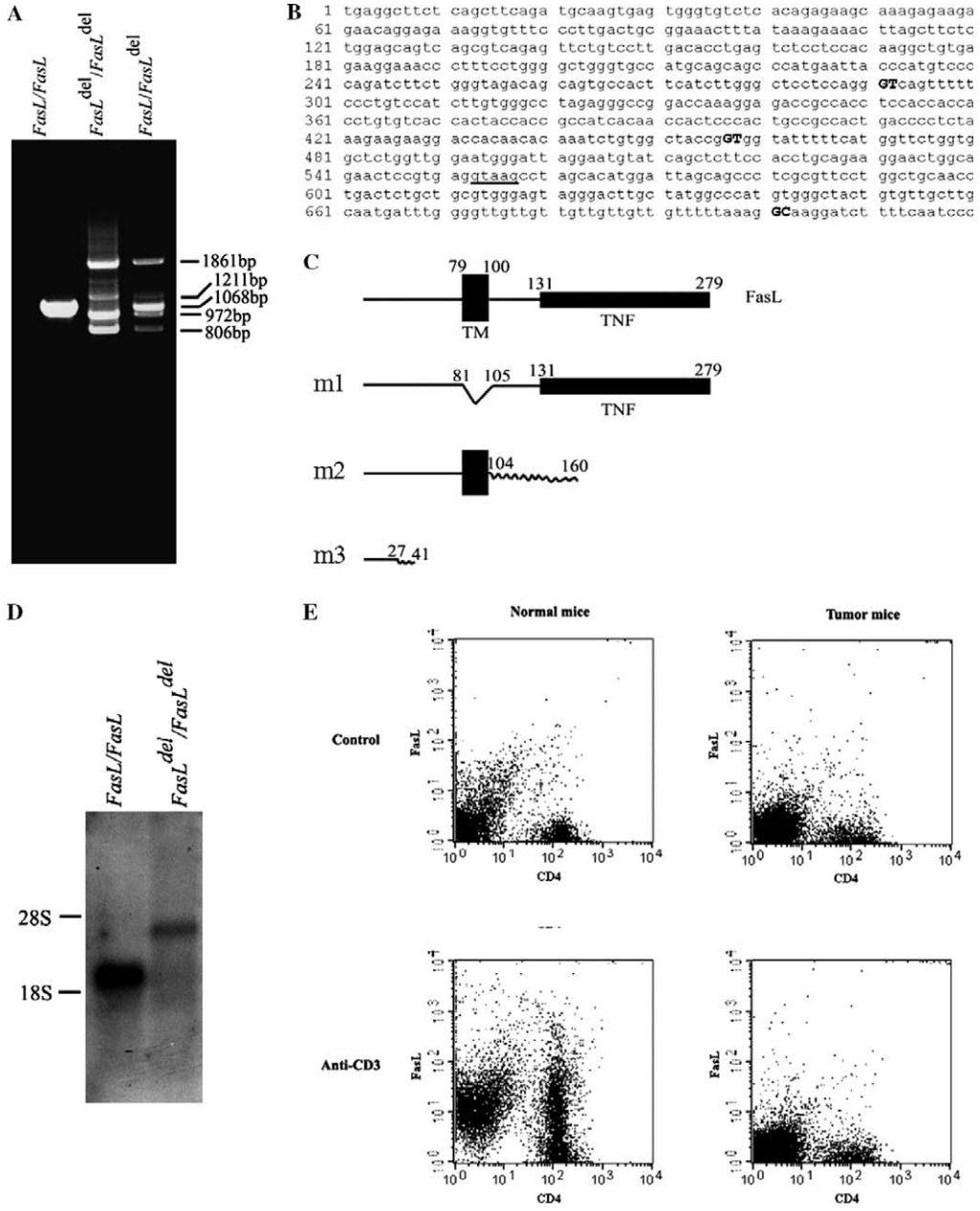

Fig. 6. Loss-of-function of FasL in lymphoma mice. (A) RT-PCR results showing the aberrant transcripts in homozygous and heterozygous mutant mice. (B) Partial sequence of *FasL* showing the three cryptic splicing sites (GT and GC in upper case and bold) that are employed in mutant mice. The 1068 bp fragment is derived from normally spliced mRNA, while 1861 bp fragment is the unspliced transcript retaining intron 1. The 1211 bp fragment is derived from the use of cryptic splicing donor site (GC) within the intron 1. The 972 and 860 bp fragments are derived from splicing using the second and first cryptic (GT) splicing donor site within exon 1. (C) Comparison of predicted polypeptides that might be produced from the aberrant transcripts with the wild-type FasL. The m1 polypeptide without the transmembrane domain (TM) is derived from the 972 bp transcript, while m2 is generated from 1861 and 1211 bp transcripts and m3 mutant polypeptide is predicted to be a product of the 860 bp transcript. The waved-lines represent peptides that are not homologous with the wild-type FasL. (D) Northern blotting showing that the major transcript in tumor mice is the one with the first intron retained (unspliced). (E) Flow cytometry analysis of FasL expression on splenic T lymphocytes. T cells were cultured for 7 h on anti-CD3-coated or uncoated control plates before being subjected to FACS analysis for surface CD4 and FasL. The anti-CD3 antibody stimulated expression of FasL above background in normal T cells but not in T cells derived from tumor mice.

were apparently all Fas-positive. When gated at 10^2, less than 3% versus more than 25% splenocytes were Fas-positive in normal and tumor mice, respectively. Interestingly, there were about 6–10% of Fas-high but $CD3^-$ or $B220^-$ cells in tumor mice, suggesting that the Fas–FasL signaling does not solely target the $CD3^+B220^+$ population. Actually, it has been reported in the FasL-null mice that normal T cells and B cells are also increased although not to the extent of the $CD3^+B220^+$ cells [10].

Discussion

We have described here a novel spontaneous mutation in the mouse *FasL* gene and we have shown that it is a

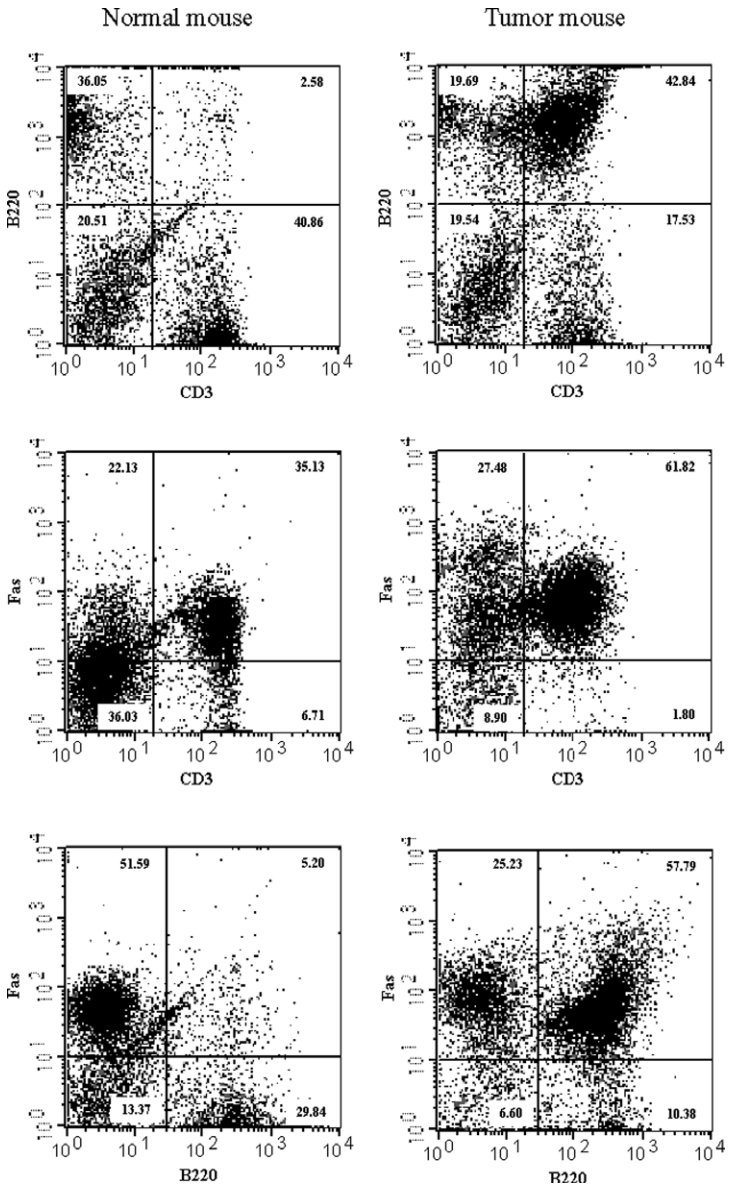

Fig. 7. Increased expression of Fas on tumor splenocytes. Splenocytes from a pair of 4-month-old female mice were stained for CD3, B220 and Fas and scanned with a flow cytometry. There were more cells expressing higher levels of Fas in cells derived from the tumor mouse than the normal mouse and the CD3 and B220-double-positive cells were Fas-positive.

small deletion of five nucleotides at the 5′ end of the first intron. This deletion has removed the invariant GT dinucleotide in the 5′ splice consensus sequence [18], resulting in aberrant splicing between the first and the second exons and therefore generating non-functional polypeptides. Mutations affecting splicing are not rare. It is estimated that about 15% of human genetic diseases result from splicing defects[18]. Whether or not a similar mutation in the human *FasL* exists is currently unknown.

The phenotype of our mice is very similar to that of the *FasL* knockout mice, which is much more severe than that observed in the *gld* point mutation mice, suggesting that this new mutation is a complete loss-of-function of the *FasL* gene. However, unlike the knockout allele that has lost more than 10 kb and therefore might potentially perturb the functions of neighboring genes, our $FasL^{del}$ allele is a tiny deletion whose effect on other genes is minimized. In contrast to earlier studies, in which there is no thymic defect reported for either *Fas* or *FasL* knockout mice [8–10], we found that $FasL^{del}/FasL^{del}$ thymuses were massively infiltrated with $CD3^{+}B220^{+}$ cells, leading to enlargement of the thymus at later ages. We believe that this phenotype might have been overlooked in *Fas* and *FasL* knockout mice since this defect manifests only in old mice. Alternatively, the thymic phenotype might be unique to the $FasL^{del}$ allele. Although the basic phenotype is indistinguishable on all genetic backgrounds, lymphoid invasion into the liver and the lungs is most prominent on the BALB/c background. This is consistent with the fact that FasL exists in two polymorphisms and the BALB/c FasL functions

more efficiently than the FasL of C3H, 129, and C57BL/6 [19].

The Fas–FasL signaling pathway has been well established as a major apoptosis pathway with conclusive in vitro and in vivo evidence. Studies in the last decade have revealed the molecular mechanism of this pathway, but the physiological significance of the Fas–FasL signaling has not been fully understood. A prevailing point is that Fas signaling functions to suppress autoimmune reactions, but the fact is that the increase of autoimmune antibodies in both Fas-null [9] and FasL-null [10] mice is proportional to the increase of total immunoglobulins, suggesting that Fas signaling functions to control the quantity of total immunoglobulins rather than to particularly suppress autoimmune antibodies. The hall marker of disruption of FasL–Fas signaling is the dramatic expansion of the $CD3^{+}B220^{+}$ population of lymphocytes, but the function of these cells in immunity remains unknown and they are still considered to be ''futile'' or ''abnormal'' cells for the time being. When, where, and how these cells are generated in vivo are not clear ether. A possible role of FasL–Fas signaling in tumor surveillance also remains to be proven [20]. The mutant mice we described here might be a good animal model to further our understanding of functions of the FasL–Fas signaling pathway.

Acknowledgment

This work was funded by the Singapore Agency for Science, Technology and Research (A*STAR).

References

[1] T. Suda, T. Takahashi, P. Golstein, S. Nagata, Molecular cloning and expression of the Fas ligand, a novel member of the tumor necrosis factor family, Cell 75 (1993) 1169–1178.
[2] S. Nagata, P. Golstein, The Fas death factor, Science 267 (1995) 1449–1456.
[3] F.C. Kischkel, S. Hellbardt, I. Behrmann, M. Germer, M. Pawlita, P.H. Krammer, M.E. Peter, Cytotoxicity-dependent APO-1 (Fas/CD95)-associated proteins form a death-inducing signaling complex (DISC) with the receptor, EMBO J. 14 (1995) 5579–5588.
[4] K. Boatright, M. Renatus, F. Scott, S. Sperandio, H. Shin, I. Pedersen, J. Ricci, W. Edris, D. Sutherlin, D. Green, A unified model for apical caspase activation, Mol. Cell 11 (2003) 529–541.
[5] S.T. Ju, D.J. Panka, H. Cui, R. Ettinger, M. el-Khatib, D.H. Sheer, B.Z. Stanger, A. Marshak-Rothstein, Fas(CD95)/FasL interactions required for programmed cell death after T-cell activation, Nature 373 (1995) 444–448.
[6] S.E. Straus, E.S. Jaffe, J.M. Puck, J.K. Dale, K.B. Elkon, A. Rösen-Wolff, A.M.J. Peters, M.C. Sneller, C.W. Hallahan, J. Wang, R.E. Fischer, C.M. Jackson, A.Y. Lin, C. Bäumler, E. Siegert, A. Marx, A.K. Vaishnaw, T. Grodzicky, T.A. Fleisher, M.J. Lenardo, The development of lymphomas in families with autoimmune lymphoproliferative syndrome with germline Fas mutations and defective lymphocyte apoptosis, Blood 98 (2001) 194–200.
[7] T.S. Griffith, T. Brunner, S.M. Fletcher, D.R. Green, T.A. Ferguson, Fas ligand-induced apoptosis as a mechanism of immune privilege, Science 270 (1995) 1189–1192.
[8] M. Adachi, S. Suematsu, T. Kondo, J. Ogasawara, T. Tanaka, N. Yoshida, S. Nagata, Targeted mutation in the Fas gene causes hyperplasia in peripheral lymphoid organs and liver, Nat. Genet. 11 (1995) 294–300.
[9] M. Adachi, S. Suematsu, T. Suda, D. Watanabe, H. Fukuyama, J. Ogasawara, T. Tanaka, N. Yoshida, S. Nagata, Enhanced and accelerated lymphoproliferation in Fas-null mice, Proc. Natl. Acad. Sci. USA 93 (1996) 2131–2136.
[10] S. Karray, C. Kress, S. Cuvellier, C. Hue-Beauvais, D. Damotte, C. Babinet, M. Lévi-Strauss, Complete loss of Fas ligand gene causes massive lymphoproliferation and early death, indicating a residual activity of gld allele, J. Immunol. 172 (2004) 2118–2125.
[11] T. Takahashi, M. Tanaka, C.I. Branna, N.A. Jenkins, N.G. Copeland, T. Suda, S. Nagata, Generalized lymphoproliferative disease in mice, caused by a point mutation in the Fas ligand, Cell 76 (1994) 969–976.
[12] M. Adachi, R. Watanabe-Fukunaga, S. Nagata, Aberrant transcription caused by the insertion of an early transposable element in an intron of the Fas antigen gene of lpr mice, Proc. Natl. Acad. Sci. USA 90 (1993) 1756–1760.
[13] R. Watanabe-Fukunaga, C.I. Brannan, N. Itoh, S. Yonehara, N.G. Copeland, N.A. Jenkins, S. Nagata, Lymphoproliferation disorder in mice explained by defects in Fas antigen that mediates apoptosis, Nature 356 (1992) 314–317.
[14] G.H. Fisher, F.J. Rosenberg, S.E. Straus, J.K. Dale, D.L. Middleton, A.Y. Lin, W. Strober, M.J. Lenardo, J.M. Puck, Dominant interfering Fas gene mutations impair apoptosis in a human autoimmune lymphoproliferative syndrome, Cell 81 (1995) 935–946.
[15] C.E. Jackson, R.E. Fischer, A.P. Hsu, S.M. Anderson, Y. Choi, J. Wang, J.K. Dale, T.A. Fleisher, L.A. Middelton, M.C. Sneller, M.J. Lenardo, S.E. Straus, J.M. Puck, Autoimmune lymphoproliferative syndrome with defective Fas: genotype influences penetrance, Am. J. Hum. Genet. 64 (1999) 1002–1014.
[16] R.M. Siegel, J.R. Muppidi, M. Sarker, A. Lobito, M. Jen, D. Martin, S.E. Straus, M.J. Lenardo, SPOTS: signaling protein oligomeric transduction structures are early mediators of death receptor-induced apoptosis at the plasma membrane, J. Cell Biol. 167 (2004) 735–744.
[17] J. Roesler, J.M. Izquierdo, M. Ryser, A. Rösen-Wolff, M. Gahr, J. Valcarce, M.J. Lenardo, L. Zheng, Haploinsufficiency, rather than the effect of an excessive production of soluble CD95 (CD95{Delta}TM), is the basis for ALPS Ia in a family with duplicated 3′ splice site AG in CD95 intron 5 on one allele, Blood 106 (2005) 1652–1659.
[18] M. Krawczak, J. Reiss, D.N. Cooper, The mutational spectrum of single base-pair substitutions in mRNA splice junctions of human genes: causes and consequences, Hum. Genet. 90 (1992) 41–54.
[19] N. Kayagaki, N. Yamaguchi, F. Nagao, S. Matsuo, H. Maeda, K. Okumura, H. Yagita, Polymorphism of murine Fas ligand that affects the biological activity, Proc. Natl. Acad. Sci. USA 94 (1997) 3914–3919.
[20] M.E. Peter, P. Legembre, B.C. Barnhart, Does CD95 have tumor promoting activities? Biochim. Biophys. Acta 1755 (2005) 25–36.
[21] C.-C. Wang, C.P. Ng, L. Lu, V. Atlashkin, W. Zhang, L.F. Seet, W. Hong, A role of VAMP8/endobrevin in regulated exocytosis of pancreatic acinar cells, Dev. Cell 7 (2004) 359–371.